24th ABCM International Congress of Mechanical Engineering
December 3-8, 2017, Curitiba, PR, Brazil

COBEM-2017-1643
THERMODYNAMIC ANALYSIS OF ADIABATIC COMPRESSED AIR ENERGY STORAGE SYSTEMS

Tomás Pessoa Londe Camargos
Programa de pós-graduação da Universidade Federal de Minas Gerais, Belo Horizonte, Brasil
tomascamargos@yahoo.com.br

Daniel Leon Ferreira Pottie
Laboratório de Termometria da Universidade Federal de Minas Gerais, Belo Horizonte, Brasil
d.pottie@gmail.com

João Vítor de Navarro Moreira
Programa de pós-graduação da Universidade Federal de Minas Gerais, Belo Horizonte, Brasil
joaovitornavarro@gmail.com

Glycon Pena de Souza Barros
Fluenge Engenharia, Belo Horizonte, Brasil
glycon.barros@fluenge.com.br

Matheus Pereira Porto
Departamento de Engenharia Mecânica, Universidade Federal de Minas Gerais, Belo Horizonte, Brasil
matheuspporto@ufmg.br

Abstract. *This article purpose is the development a thermodynamic model that simulates the performance of a Compressed Air Energy Storage System, during its charging stage. In this phase, the irreversibilities considered were due to the heat exchange between the compressor housing and the surrounding environment. The air storage tank was considered adiabatic though. The pressurizing stage was analyzed as a transient process, as a consequence of the variable inlet mass flow. Therefore, through the simulation the behavior of several variables involved in the process were assessed (e.g. pressure, temperature, compressor work and the irreversibilities). This analysis made it possible to quantify the amount of energy that can be stored in a reservoir and also the exergy destroyed during the air storage process.*

Keywords: *Compressed air energy storage, thermodynamics, charging stage.*

1. INTRODUCTION

A compressed air energy storage (CAES) system is one in which some kind of available excess power is used, during periods of lower power demands, to drive a compressor that in turn, pressurizes air into an artificial or natural storage cavern. The pressure is eventually released through a proper device, and thus, energy is recovered to be used during periods of peak demand of electricity. According to Schoenung (2001), CAES systems are one of the most reliable technologies for large-scale energy storage, with efficiency varying from 66 up to 82% (Succar and Williams, 2008).

Currently there are two large scale CAES plants in operation in the world. One is in Hunford, Germany, with a capacity of 321 MW, and the other is in McIntosh, Alabama, USA, with an installed capacity of 110 MW.

In this scenario, it is important to be determine the performance of CAES systems so that they can be properly compared to other storage alternatives. To do so, several thermodynamic models have been proposed intending to describe the behavior and interdependency of some of the variables involved in the process. Najjar and Zaamout (1998) and Lund, *et al.*, 2009, neglected any effects the storage cavern may have on the system. Grazzini and Milazzo, (2008), Grazzini and Milazzo, (2012) and Yang, *et al.*, 2014, considered that the temperature of the air in the storage cavern remains constant. Osterle (1991) and Hartmann, *et al.*, 1987, analyzed the system considering adiabatic storage.

In this work, a thermodynamic model was developed emphasizing on the CAES charging stage. A major consideration made in this model is that the air storage reservoir would be adiabatic. The mass flow rate, which is generally considered constant in the majority of the available literature, varied during the process, reducing as the pressure on the reservoir increases. In order to evaluate the energy that can be stored in the compressed air tank, as well as the exergy destroyed during the charging stage, several graphs have been generated and they are presented in the upcoming section 3.

2. METHODOLOGY

To implement the thermodynamic routine in MATLAB a real compressor was used as reference. Its technical data are presented on the following Tab.1

Table 1. Compressor data sheet.

Parameter	Value
Power	3,75 kW
Swept volume	593 cm^3
Clearance – ε	0,0069213
Maximum reservoir pressure	970 kPa
Reservoir volume	0,202 m^3

Each cycle was determined as the time it takes for a piston of the compressor to move from the bottom dead centre (BDC) to the top dead centre (TDC) and come back all the way through. When the referred cylinder returns to the BDC, another cycle begins. The sub-indexes *i* and *f* respectively indicate the *beginning* and *end* of a cycle, while the sub-indexes *c* and *r* indicate both the compressor *cylinder chamber* and the *reservoir*, respectively.

The modeling of the charging stage of the CAES system was performed through an iterative process through Eq. (1) to (7), in which the first step consists in calculating the volumetric efficiency of compression η_v, by the following equation:

$$\eta_v = 1 + \varepsilon - \varepsilon \cdot \left(\frac{P_{f\text{-}c}}{P_{i\text{-}c}}\right)^{\frac{1}{n}} \tag{1}$$

Where ε represents the compressor clearance; *n* is the dimensionless polytropic coefficient; P_{i-c} is the initial compression pressure, considered equal to the local atmospheric pressure (92 kPa); P_{f-c} is the final compression pressure - considered equal to the pressure in the reservoir at the end of the compression (P_{f-r}), in kPa.

For the first calculation of P_{f-c}, its value was estimated to be 15% greater than P_{f-r} (92 kPa). The calculation then proceeds, cycling from (1) to (7) until the values of P_{f-c} and P_{f-r} converge with an error of 0.1% between them.

Holding the volumetric efficiency value, the iterative process proceeds. The next stage consists on the mass flow rate $\dot{m}_{air}$ calculation, for each cycle, as follows:

$$\dot{m}_{air} = N \cdot V_s \cdot \rho_{air} \cdot \eta_v \tag{2}$$

In which the axis rotation N is given in rpm, V_s is the swept volume, in cm³ and ρ_{ar} is the specific mass of the air at ambient conditions [kg m^{-3}].

The final compression temperature T_{f-c} was calculated by the polytropic process equation, in which T_{i-c} represents the initial compression temperature, all given in K:

$$\frac{T_{f\text{-}c}}{T_{i\text{-}c}} = \left(\frac{P_{f\text{-}c}}{P_{i\text{-}c}}\right)^{\frac{n-1}{n}} \tag{3}$$

The initial mass m_{i-r} in the reservoir of each cycle has been calculated by the ideal gas law. In the first cycle, the initial reservoir air temperature – T_{i-r} – was considered equal to 298K; V_r is the reservoir volume, in m³ and R_{air} is the ideal gas constant for air, with a value of 0.287 kJ kg^{-1} K^{-1}. Therefore:

$$m_{i\text{-}r} = \frac{P_{i\text{-}r} \cdot V_r}{R_{ar} \cdot T_{i\text{-}r}} \tag{4}$$

Then, the final temperature of the reservoir $T_{f\text{-}r}$ was calculated through the weighted average between the mass in the reservoir at the beginning of the cycle, taken at its initial temperature, and the mass entering the reservoir during the cycle, at the final temperature of compression $T_{f\text{-}c}$:

$$T_{f\text{-}r}=\frac{T_{i\text{-}r}\cdot m_{i\text{-}r}+T_{f\text{-}c}\cdot m_e}{m_{i\text{-}r}+m_e} \tag{5}$$

In which the entering mass m_e during a cycle corresponds to the mass flow rate $\dot{m}_{air}$, as both have been taken with a single cycle time-span reference. Thus being, the final mass in the reservoir is represented by:

$$m_{f\text{-}r}=m_{i\text{-}r}+m_e \tag{6}$$

Finally, the pressure inside the reservoir in the end of a single compression cycle can then be calculated, by making use of the ideal gases law once again:

$$P_{f\text{-}r}=\frac{m_{f\text{-}r}\cdot R_{air}\cdot T_{f\text{-}r}}{V_r} \tag{7}$$

Here, the value of $P_{f\text{-}r}$ is then compared to $P_{f\text{-}c}$, and if its values diverge by more than 0.1%, the simple iterative process returns to Eq. (1), decreasing $P_{f\text{-}c}$ by 0.001, and the looping process restarts. When convergence criterium is reached, the iterative process ends.

The modeling then continues, by determining the work made and the heat released during the compression, for each cycle, as proposed by Costa, 1978:

$$\dot{W}_c=\frac{\dot{m}_{air}\cdot R_{air}\cdot\left(T_{f\text{-}c}-T_{i\text{-}c}\right)}{1\text{-}n} \tag{8}$$

$$\dot{Q}_c=\dot{m}_{air}\cdot\left(\frac{k\text{-}n}{1\text{-}n}\right)\cdot c_v\cdot\left(T_{f\text{-}c}-T_{i\text{-}c}\right) \tag{9}$$

Where k is the dimensionless isentropic coefficient (with a value of 1.4) and c_v is the specific heat at constant volume, given in kJ kg^{-1} K^{-1}. The entropy variation – $\Delta\dot{S}_c$ – for the air in the cylinder chamber, during the compression, was calculated as follows:

$$\Delta\dot{S}_c=\dot{m}_{air}\left[c_p\cdot ln\left(\frac{T_{f\text{-}c}}{T_{i\text{-}c}}\right)\text{-}R_{air}\cdot ln\left(\frac{P_{f\text{-}c}}{P_{i\text{-}c}}\right)\right] \tag{10}$$

In which the entropy variation is given in kJ K^{-1} and c_p is the specific heat at constant pressure, in kJ kg^{-1} K^{-1}.

The generation of entropy $\dot{S}_{gen}$ [kJ K^{-1}] can be calculated through the 2nd law of thermodynamics, where T_∞ represents the surrounding environment temperature, in K.

$$\dot{S}_{gen}=\Delta\dot{S}_c\text{-}\frac{\dot{Q}_c}{T_\infty} \tag{11}$$

Thus, the irreversibility generation rate [kJ/cycle] can be obtained by:

$$\dot{I}=T_\infty\cdot\dot{S}_{gen} \tag{12}$$

Finally, the exergy in the reservoir was calculated as follows:

$$X_r=m_{f-r}\left[\left(u_f\text{-}u_0\right)+P_0\left(v_f\text{-}v_0\right)\text{-}T_0\left(s_f\text{-}s_0\right)\right] \tag{13}$$

In which the u represents the internal energy [kJ/kg], v is the specific volume, in m³ kg^{-1}, P is the pressure [kPa], T is the temperature [K] and s is the specific entropy [kJ kg^{-1} K^{-1}]. The sub-index 0 indicates that the property should be evaluated in the ambient state and the f subscript represent the end of a single cycle.

3. RESULTS AND DISCUSSION

Through the routine made in MATLAB described above, it was possible to graphically visualize the behavior of each of the variables of the system. Figure 1 shows the pressure in the reservoir throughout the charging stage. The consistency observed in the curve slope is due to the pressure increasing steadily, even though the mass flow ratio decreases over time. This resulted on an almost linear behavior for the reservoir pressure over time.

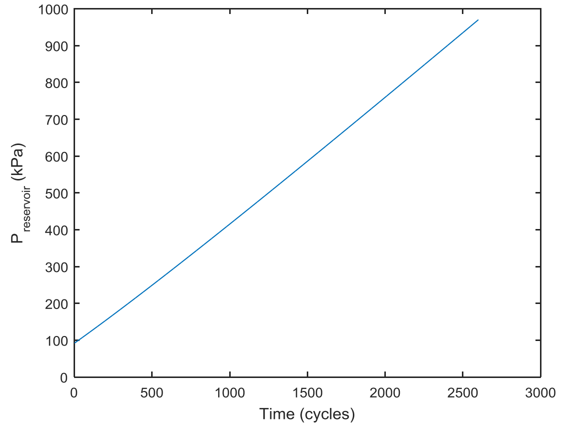

Figure 1. Behavior of the pressure in the reservoir of the CAES system.

Figure 2 shows the behavior of the mass flow rate over time. It is possible to notice that this variable value decreases over the charging stage, as the pressure in the reservoir increases, resulting in more resistance to the incoming mass entering the chamber.

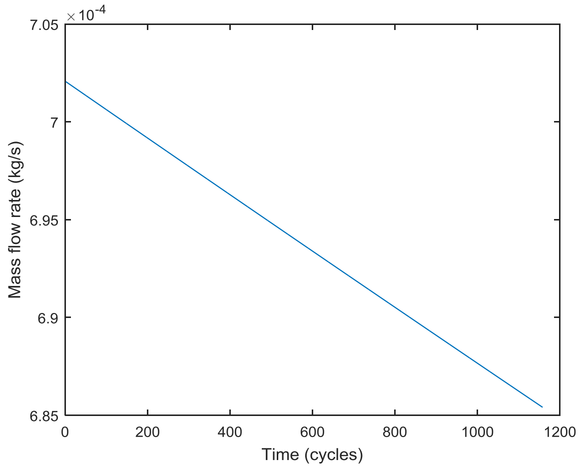

Figure 2. Mass flow rate throughout the charging stage of the CAES system.

Next, Fig. 3 shows the temperature of the air in the reservoir over time. The temperature in the cavern increases non-linearly due to the final compression temperature - $T_{f\text{-}c}$ - getting higher by each cycle, which in turn, can be observed in Fig. 4.

The temperature at the end of the compression, $T_{f\text{-}c}$ increases because the final pressure keeps getting higher, to match the also increasing reservoir pressure, whilst its initial state remains the same (ambient pressure and temperature). This means that as the cycling proceed, the required work grows and consequently, the final temperature achieved also builds up. This behavior was expected, as shown by Eq. (3).

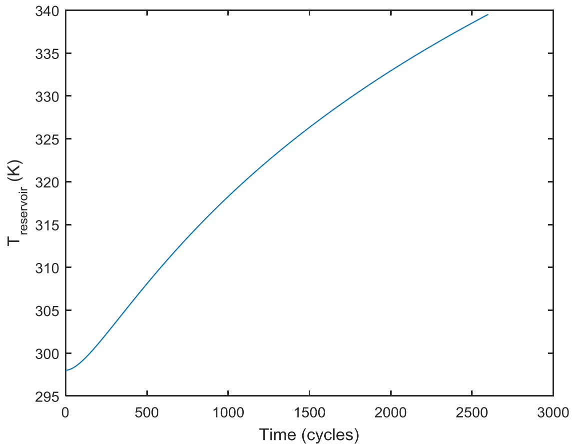

Figure 3. Temperature profile in the reservoir of the system.

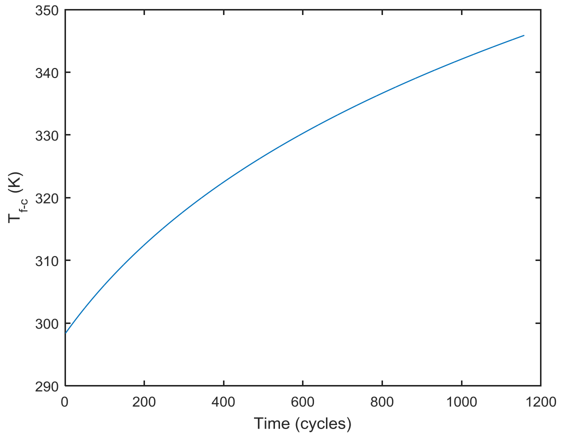

Figure 4. Behavior of final compression temperature.

Figures 5 and 6 represent, respectively, the heat generated and work consumed during compression. The negative values are consistent with the sign convention proposed in the literature (Çengel and Boles, 2001). It is possible to notice that the compression work increases throughout the charging stage, as previously explained. The heat generated, and then exchanged by the compressor to the surrounding environment also grows as the final compression temperature increases, and thus, the external surface of the cylinder's chamber of the compressor.

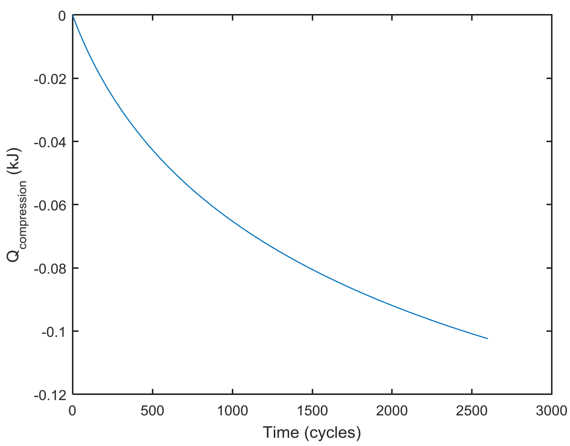

Figure 5. Heat generated and exchanged by the compressor and the environment during compression.

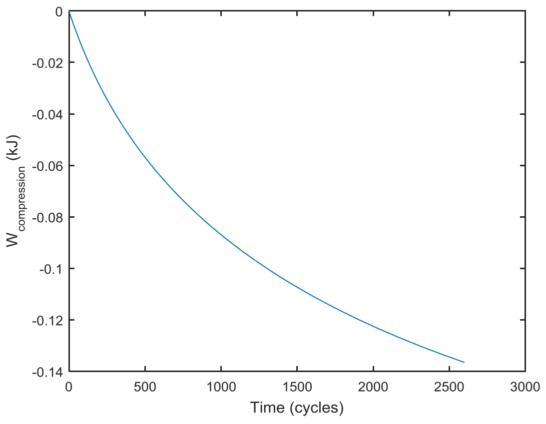

Figure 6. Compression work behavior throughout the charging stage of the CAES system.

The irreversibility due to the heat exchange between the compressor and the environment is shown in Fig. 7. The irreversibility increases with time in an almost linear manner, due to the increase in the heat exchange Q_c and the entropy change.

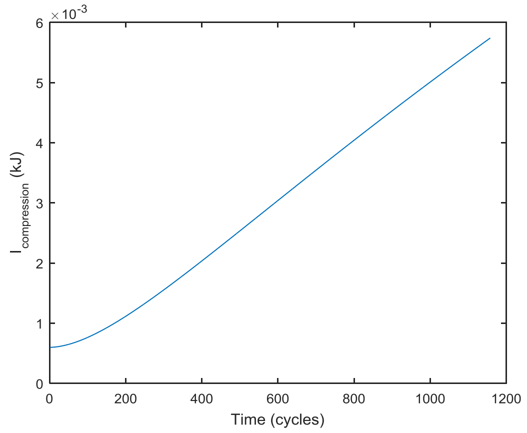

Figure 7. Behavior of irreversibility due to heat exchange between the compressor and the environment.

Figure 8 shows the exergy stored in the reservoir along the charging stage. The profile of the exergy curve is consistent with the profile of both pressure and temperature curves (by Fig. 1 and 3, respectively). It also can be seen that the exergy increases less significant in the final of the charging, as a consequence of the difficulty of adding mass in the reservoir, when it is almost fully loaded.

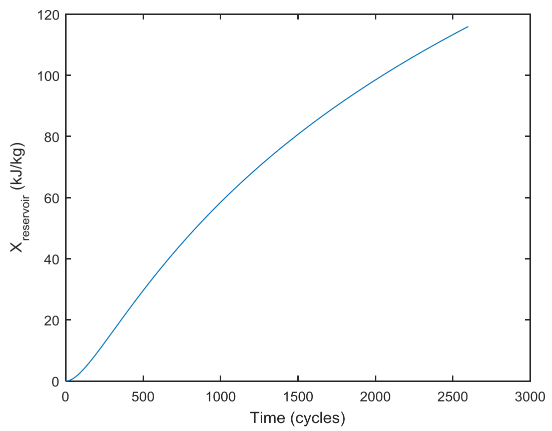

Figure 8. Behavior of the exergy in the reservoir of the CAES system.

4. CONCLUSONS

This work consisted on the elaboration of a thermodynamic model that simulates the behavior of the variables involved in the processes. It was also possible to evaluate the amount of energy that can be stored in the described CAES system, as well as the irreversibilities present in the process. The generated graphs are consistent with the equations and provide a quick understanding of the performance of the variables, making possible to design a CAES system to work with minimum entropy generation.

It is expected with the development of this work, perform system validations with an experimental set-up. This validated project can serve as a reference in the design of a higher scale CAES system.

Charging time is an important variable, since solar variability may limit the time at which the device is to be charged. It is hoped that the development of this research will present new management strategies for this form of storage in order to mitigate the variability of photovoltaic generation.

5. ACKNOWLEDGEMENTS

This work was supported by CNPQ and Federal University of Minas Gerais (UFMG).

6. REFERENCES

Çengel, Y.A. and Boles, M.A., 2001. *Thermodynamics: an engineering approach*. Boston, McGraw-Hill.

Costa, E.C., 1978. *Compressores*. São Paulo: Edgard Blucher.

Grazzini, G. and Milazzo, A., 2012. A thermodynamic analysis of multistage adiabatic CAES. *Proc IEEE 2012*;100:461e72.

Grazzini, G. and Milazzo, A., 2008. Thermodynamic analysis of CAES/TES systems for renewable energy plants. *Renew Energy 2008*;33:1998e2006.

Hartmann, N., V€ohringer, O., Kruck, C. and Eltrop, L., 2012. Simulation and analysis of different adiabatic compressed air energy storage plant configurations. *Appl Energy 2012*;93:541e8. Including Unsteady Effects". Anaheim, CA, USA, 1987. 10 p.

Lund, H., Salgi, G., Elmegaard, B. and ANDERSEN, A. N., 2009. Optimal operation strategies of compressed air energy storage (CAES) on electricity spot markets with fluctuating prices. *Appl Therm Eng 2009*;29:799e806.

Najjar, Y.S.H and Zaamout M.S., 1998. Performance analysis of compressed air energy storage (CAES) plant for dry regions. *Energy Convers Manage 1998*;39: 1503e11.

Osterle, J.F., 1991. The thermodynamics of compressed air exergy storage. *J Energy Resour Technol*.

Schoenung, S.M., 2001. Characteristics and technologies for long- vs. short-term energy storage. *Sandia Rep. SAND2001-0765*.

Succar, S. and Williams, R.H., 2008. Compressed air energy storage: theory, resources, and applications for wind power. *Princet Environ Inst Rep*.

Yang, Z.W., Wang, Z., Ran, P., Li, Z. and Ni, W.D., 2014. Thermodynamic analysis of a hybrid thermal-compressed air energy storage system for the integration of wind power. *Appl Therm Eng 2014*;66:519e27.

7. RESPONSIBILITY NOTICE

The authors are the only responsible for the printed material included in this paper.